Geologica Acta: an international earth science journal
ISSN: 1695-6133
geologica-acta@ija.csic.es
Universitat de Barcelona
España

MATTIA, M.; BRUNO, V.; CANNAVÒ, F.; PALANO, M.
Evidences of a contractional pattern along the northern rim of the Hyblean Plateau (Sicily, Italy) from GPS data
Geologica Acta: an international earth science journal, vol. 10, núm. 1, 2012, pp. 1-8
Universitat de Barcelona
Barcelona, España

Geologica Acta, Vol.10, Nº 12, March 2012, 1-8
DOI: 10.1344/105.000001705
Available online at www.geologica-acta.com

Evidences of a contractional pattern along the northern rim of the Hyblean Plateau (Sicily, Italy) from GPS data

M. MATTIA [1] [*] **V. BRUNO** [1] **F. CANNAVÒ** [1] **M. PALANO** [1]

[1] **Istituto Nazionale di Geofisica e Vulcanologia, Sezione di Catania**
Piazza Roma 2, 95123 Catania, Italy Mattia E-mail: mario.mattia@ct.ingv.it

[*] Corresponding author, Tel. +39. 95.7165805 Fax. +39. 95.435801

ABSTRACT

In this paper we present the main results inferred from GPS data collected between 1998.00 and 2009.78 along the northern rim of the Hyblean Plateau from 9 continuous and 23 survey-mode sites. From a geological point of view, this area is of great interest because 1) it represents an important piece of the collision front between Nubia and Eurasia 2) it is very close to the biggest European volcano Mount Etna and 3) it has been hit by strong earthquakes in the past (1169 and 1693) that struggled the cities of Catania, Siracusa and Ragusa provoking tens of thousands of casualties. We have found that the ground deformation pattern clearly defines an area of prevailing contraction along the northern rim of the Hyblean Plateau with a maximum negative strain-rate of about 0.14µstrain/yr in agreement with both geological and Interferometric Synthetic Aperture Radar (InSAR) data. In addition, a transition to extensional regime is acting toward the central sector of the plateau. The velocity field referred to the Eurasian frame indicates that a large part of the plateau is dominated by a 5.4mm/yr northward motion.

KEYWORDS **Hyblean Plateau. GPS. Active tectonics. Deformation. Geodynamic.**

INTRODUCTION

Southern Italy is a key area for understanding the tectonic processes due to the ~N20°W Neogene-Quaternary convergence between Nubia and Eurasia. Geodetic studies have demonstrated that most of Sicily moves together with the Nubian plate (the African plate west of the East African Rift), as GPS velocities at stations in Sicily match the Nubian plate motion (e.g. Hollestein et al., 2003; D'Agostino and Selvaggi, 2004; Serpelloni et al. 2007). Although recent papers (Serpelloni et al., 2007) evidence that there is a motion relative to the Nubian plate at some sites in internal Sicily probably related to the opening of the Sicily Channel rift zone (D'Agostino et al., 2008), there is a general agreement around the concept that the internal deformation in Sicily is small (except on its north-eastern corner) and the Eurasia-Nubia convergence appears to be absorbed in a belt located north of Sicily and south of Ustica (Fig. 1A). This offshore zone is characterized by frequent, moderate-sized thrust earthquakes having focal mechanisms with NNW-SSE and NW-SE compressive axes (Fig. 1A; see Mattia et al., 2009 for details and references therein).

Here, we analyzed the horizontal ground deformation pattern in terms of velocity field (referred to a Eurasian reference frame) and strain-rate field through the processing of episodic and continuous GPS data collected between 1998.00 and 2009.78 on a dense network established along the northern rim of the Hyblean Plateau (Fig. 1B). Our findings are in agreement with both geological and geophysical data in evidencing an active contractional process along the northern rim of Hyblean Plateau, suggesting that part of the Eurasia-Nubia convergence could be adsorbed on this area.

BACKGROUND SETTING

The Hyblean Plateau lying in the south-eastern part of Sicily is part of the Tertiary orogenic foreland slightly deformed by the Eurasia-Nubia convergence process (Barberi et al., 1973; Boccaletti and Manetti, 1978; Patacca et al., 1990; Doglioni et al., 1999). To the east, the plateau is bounded by the NNW-SSE Hyblean-Maltese escarpment (Fig. 1B), one of the largest normal fault systems of the Mediterranean basin, which separates the thick inland continental crust from the Ionian Mesozoic oceanic crust (e.g., Reuther et al., 1993; Adam et al., 2000). The northern and western margins of the Hyblean Plateau are characterized by an older extensional belt (named Gela-Catania Foredeep; Fig. 1B), that forming a roughly NE-SW alignment, is downbent by a NE-SW fault system under the front of the Appennine-Maghrebian chain (Yellin-Dror et al., 1997).

Two main extensional NE-SW-oriented basins can be recognized along the Gela-Catania Foredeep: the Scordia-Lentini Graben, to the north, and the Marina di Ragusa Graben to the south (Grasso and Reuther, 1988; Grasso et al., 2000). Both tectonic depressions, filled with Quaternary sedimentary deposits, are linked by a roughly N-S oriented fault system named Scicli-Ragusa fault system (Ghisetti and Vezzani, 1980; Grasso and Reuther, 1988). Recent studies (Bousquet and Lanzafame, 2004; Catalano et al., 2006, 2008) have demonstrated that since about 0.85Ma, the normal faults controlling the Scordia-Lentini and the Marina di Ragusa extensional basins as well as the fault segments of the Scicli-Ragusa fault system, have been partially reactivated by reverse and left-lateral motions, respectively.

Since 1994 more than 450 earthquakes (M>1) have occurred in the area (Musumeci et al., 2005; Scarfì et al., 2007). According to Bianca et al. (1999) and Azzaro and Barbano (2000), the Hyblean-Maltese escarpment system is responsible for the primary seismic activity of the region. Major historically (4 February 1169, 11 January 1693) destructive earthquakes (M=7) occurred along this fault system (Azzaro and Barbano, 2000), causing tens of thousands of casualties. Weaker shocks (M<6) are due to secondary inland faults striking along an overall NE-SW and NNE-SSW direction (e.g., Scordia-Lentini Graben, Rosolini-Pozzallo and Scicli-Ragusa fault systems; Fig. 1B). Zones characterized by nil seismicity may be observed in

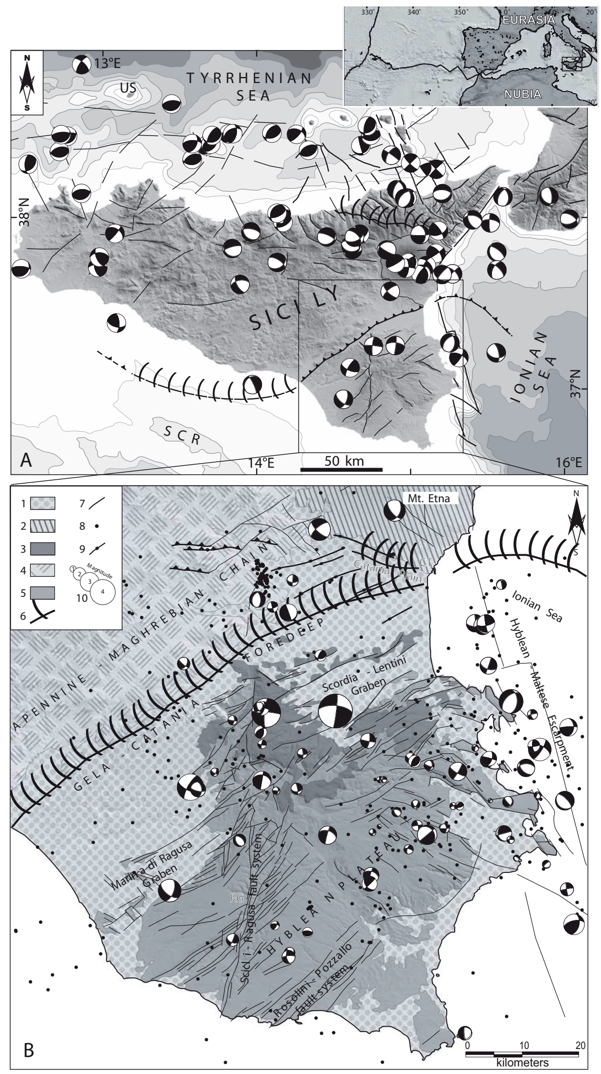

FIGURE 1 | **A) Regional tectonic map of the Southern Italy. Focal mechanisms of earthquakes (M≥3.5; depth <40km) are redrawn from Mattia et al. (2009). Abbreviations are as follow: US: Ustica; SCR: Sicily Channel Rift. The inset shows the Eurasia-Nubia plate tectonic setting. Nubia termed the African plate west of the East African Rift. The plate boundaries are drawn from Bird, (2003). B) Structural sketch map of south-eastern Sicily. 1) Recent-Quaternary sedimentary deposits; 2) Late Pleistocene-Holocene Etnean volcanics; 3) Plio-Pleistocenic Hyblean volcanics; 4) Appennine-Maghrebian units; 5) Meso-Cenozoic carbonate sediments; 6) Main thrust fronts; 7) Main faults; 8) Seismic events recorded between 1999 and 2007 (http://www.ct.ingv.it); 9) Focal mechanisms selected from Musumeci et al. (2005). Abbreviations are as follow: CT: Catania; RG: Ragusa; SI: Siracusa.**

the central part of the area. In depth, seismicity generally extends to about 30km, with foci mainly concentrated from 15 to 25km (Musumeci et al., 2005). Earthquake focal mechanisms inferred for the study area are characterized by a predominance of normal fault-plane solutions along the Hyblean-Maltese Escarpment, and mainly by strike-slip solutions with lesser amounts of both normal and reverse faulting in the plateau (Musumeci et al., 2005; Fig. 1B).

GEODETIC NETWORK AND DATA PROCESSING

GPS monitoring of the ground deformations of the Hyblean Plateau started in 1991, just after the M=5.4 1990 earthquake that struck the easternmost region of the plateau, when a GPS survey was carried out across the Scordia-Lentini Graben (Mulargia et al., 1991). The measured network partially included a local trilateration network (surveyed by Electro-optical Distance Meters technique - EDM), installed in 1991 by the International Institute of Volcanology (merged into Instituto Nazionale di Geofisica e Vulcanologia – Sezione di Catania in 2001) and a levelling route installed by the Istituto Geografico Militare Italiano (http://www.igmi.org). After 1991, the GPS network was extended and currently comprises 50 stations, including the older Electro-optical Distance Meters technique and GPS benchmarks (Fig. 2). The new geodetic monuments consist of iron and concrete pillars with a screw at the top, in order to directly install GPS antenna (Bonforte et al., 2002). In the framework of the Rete Integrata Nacionale di GPS (http://ring.gm.ingv.it) project, since 2005, the Instituto Nazionale di Geofisica e Vulcanologia – Sezione di Catania has set up 7 GPS permanent stations (afterwards GPS) improving the spatial detail of the whole Hyblean area. Since 1998, the Instituto Nazionale di Geofisica e Vulcanologia – Sezione di Catania has periodically surveyed the northern part of the network (23 benchmarks) with the aim of estimating the present day deformation of this area (Fig. 2, Table 1). GPS surveys were carried out adopting Trimble receivers (4000SSI, 4000SSE and 4700 models) and Trimble antennas (Choke Ring and Microcentered with ground plane models). Continuous GPS stations are equipped with Leica receivers (GRX1200 model) and Leica antennas (AT504 model).

All non-permanent and continuous GPS data, spanning the 1998.00 and 2009.78 time interval were processed with the GAMIT/GLOBK software packages (Herring et al., 2006a, b) with IGS (International GNSS Service - http://igscb.jpl.nasa.gov) precise ephemerides and Earth orientation parameters from the International Earth Rotation Service (http://www.iers.org) Bulletin B. In order to improve the overall configuration of the network and to combine the individual solutions in GLOBK, data from 9 continuously operating IGS stations (AJAC, CAGL, GRAS, GRAZ, LAMP, MATE, MEDI, NOT1 and NOTO; Fig. 2) were also included in the processing. The basic product of the GPS data processing are GAMIT "h-files", loosely-constrained solutions containing a set of one-day site estimate positions, Earth orientation parameters and associated error covariance matrices. Next, the individual "h-files" are combined, on a daily basis, by using the GLOBK Kalman filter with global (IGS1, IGS2, IGS3, IGS4 and EURA) solutions provided by the Scripps Orbit and Permanent Array Center (http://sopac.ucsd.edu), in order to create a daily unconstrained combined network solution. By using the GLORG module of GLOBK (Herring et al., 2006b) the loosely-constrained daily solutions were transformed into the 2005 International Terrestrial Reference Frame (ITRF2005) (Altamimi et al., 2007) and then rotated into a fixed Eurasia frame.

VELOCITY AND STRAIN-RATE FIELD

The Eurasian velocity field frame is reported in Fig. 2. The consistency between the solutions for site surveyed in campaign-mode and permanent stations can be estimated by comparing the velocities of nearby campaign and permanent site. The combined campaign-continuous velocity field shows good agreement among the elements of this combination, both in magnitude and direction of the velocity vector (Table 1). However, some variations with respect to the neighbouring stations can be observed for

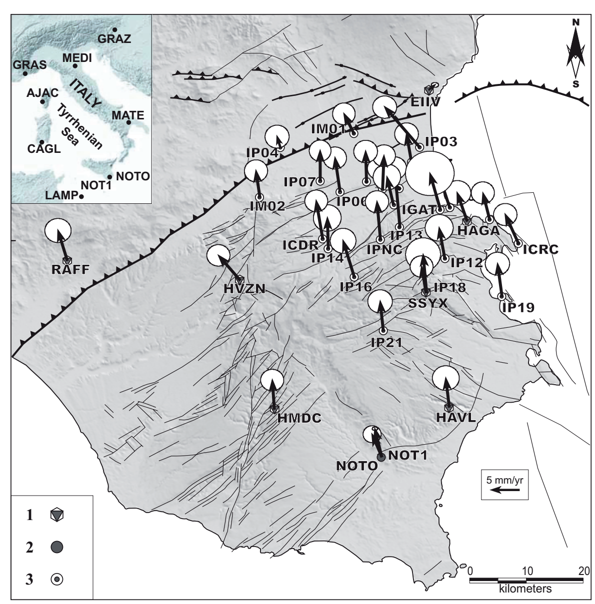

FIGURE 2 | **GPS velocities and 95% confidence ellipses in the Eurasia fixed reference frame. GPS stations analyzed in this work are reported as: 1) CGPS stations; 2) IGS stations (see inset for details); 3) GPS benchmarks surveyed in campaigns mode.**

TABLE 1 | **Site code, geodetic coordinates, East and North velocity components with associated errors for all benchmarks. Asterisks indicate the GPS sites which belong to the EUREF or IGS networks, while the black points indicate all the GPS stations that are taken into account in Fig. 5, in addition to the ones of the Hyblean Plateau. For non-permanent benchmarks the occupation time window ranges from 6 to 8 hours for each day of the surveys carried out during 1998-2000 and from 8 to 24 hours for each day of the surveys carried out during 2006. In general, the duration of each survey ranged between 5 and 10 days**

Site	Long. (deg)	Lat. (deg)	VE (mm/yr)	VN (mm/yr)
CAGL *	8.973	39.136	0.75 ± 0.14	0.41 ± 0.09
CORL ●	13.304	37.894	-0.12 ± 0.94	3.79 ± 0.86
EIIV	15.082	37.514	1.02 ± 0.25	0.86 ± 0.17
FLOR ●	14.906	37.989	-2.93 ± 1.11	2.08 ± 1.05
GRAS *	6.921	43.755	0.56 ± 0.16	0.64 ± 0.12
GRAZ *	15.493	47.067	1.11 ± 0.15	0.78 ± 0.10
HAGA	15.155	37.286	-1.69 ± 0.94	4.82 ± 0.86
HAVL	15.122	36.960	-0.59 ± 0.94	4.95 ± 0.86
HMDC	14.783	36.959	-0.34 ± 0.81	4.95 ± 0.75
HVZN	14.715	37.178	-3.67 ± 0.81	4.22 ± 0.75
IAZZ	15.048	37.380	-0.86 ± 0.83	4.90 ± 0.78
ICDR	14.876	37.249	-1.11 ± 0.80	6.52 ± 0.76
ICRC	15.256	37.241	-2.28 ± 0.82	5.02 ± 0.77
IGAT	15.105	37.299	-1.80 ± 1.70	6.21 ± 1.55
IM01	14.937	37.429	-1.69 ± 0.79	3.39 ± 0.76
IM02	14.754	37.319	-0.66 ± 0.81	4.51 ± 0.77
IMTR	15.025	37.336	-3.55 ± 0.82	3.58 ± 0.78
IP03	15.065	37.405	-5.95 ± 0.84	6.88 ± 0.78
IP04	14.794	37.405	-0.57 ± 0.84	1.90 ± 0.80
IP06	14.962	37.347	-0.16 ± 0.83	5.31 ± 0.78
IP07	14.872	37.349	-0.02 ± 0.76	5.16 ± 0.74
IP09	15.123	37.303	-1.71 ± 0.80	5.17 ± 0.76
IP10	15.201	37.282	-1.15 ± 0.81	4.56 ± 0.77
IP12	15.114	37.215	-0.97 ± 0.98	5.31 ± 0.93
IP13	15.025	37.269	-0.91 ± 0.84	10.13 ± 0.79
IP14	14.887	37.233	-0.16 ± 0.97	5.29 ± 0.93
IP16	14.938	37.184	-1.92 ± 0.90	6.22 ± 0.87
IP18	15.076	37.158	-1.11 ± 1.70	7.14 ± 1.62
IP19	15.223	37.150	-0.77 ± 0.85	5.65 ± 0.80
IP21	14.993	37.093	-0.52 ± 0.86	5.04 ± 0.81
IPNC	14.988	37.248	-0.59 ± 0.82	6.50 ± 0.77
IRNE	14.909	37.330	-0.86 ± 0.81	5.79 ± 0.77
ISCP	14.992	37.334	0.23 ± 0.80	5.73 ± 0.76
ISLI	15.015	37.308	-1.10 ± 0.96	4.74 ± 0.91
LAMP *	12.606	35.500	-2.43 ± 0.20	3.48 ± 0.13
LGUA ●	14.946	38.455	-1.88 ± 0.75	5.65 ± 0.71
MATE *	16.704	40.649	1.15 ± 0.15	4.43 ± 0.10
MILO ●	12.584	38.008	0.33 ± 0.68	2.40 ± 0.65
MM01 ●	15.501	38.171	0.66 ± 0.31	3.40 ± 0.22
MTTG ●	15.700	38.003	2.41 ± 0.96	2.27 ± 0.87
NOT1 *	14.990	36.876	-1.17 ± 0.19	4.77 ± 0.12
NOTO *	14.990	36.876	-1.65 ± 0.63	3.83 ± 0.59
RAFF	14.362	37.223	-1.58 ± 0.92	5.12 ± 0.84
RODI ●	15.167	38.108	1.40 ± 1.09	4.36 ± 1.04
SSYX	15.076	37.158	-0.76 ± 0.80	4.47 ± 0.75
TIND ●	15.036	38.138	-1.56 ± 0.69	7.26 ± 0.66
TGRC ●	15.651	38.108	1.29 ± 0.57	3.52 ± 0.54
USIX ●	13.179	38.708	0.24 ± 0.85	1.81 ± 0.79
VSER ●	14.985	38.378	-1.01 ± 0.72	9.44 ± 0.69
ZIMM *	7.465	46.877	0.71 ± 0.19	0.77 ± 0.13

some stations like IP03, IP13, IMTR, IGAT and IP18). The variations observed to these stations could be due either to site instability (outcrops of clays and volcaniclastic deposits in which the GPS benchmark was realized; IP03, IP13 and IMTR) or to a limited observation history (IGAT and IP18 were measured only in 1998 and 2000). Taking into account these observations we prefer to exclude these stations from further analysis.

The velocity field indicates that the north-eastern part of the plateau is dominated by a northward motion with an average velocity of ~5.0mm/yr according with the large, long-term tectonic structure (i.e. the Eurasia-Nubia convergence). In details, sites located close to the Gela-Catania Foredeep (EIIV, IP04, IM01) show a slight azimuthal variation coupled with lower velocity values (~2.0mm/yr) evidencing a decrease of velocity values across the foredeep, according to Bonforte et al. (2002), in which results of the GPS campaigns performed in 1998 and 2000 are analyzed. Furthermore, a local variation is observed at the HVZN station, which is installed close to the Scicli-Ragusa fault system and whose motion could be influenced by elastic strain accumulation on this fault. More north-westward, although it is located a few kilometers north of the foredeep, the RAFF station (Fig. 2), shows a velocity value close to the ones observed on the remaining part of the plateau rather than to the ones observed across the foredeep.

The horizontal strain-rate field was computed taking into account the method proposed in Haines and Holt (1993) and improved by Holt and Haines (1995), which adopts a spherical geometry by using a bi-cubic Bessel interpolation on a curvilinear grid with knots of variable spacing. Following this method (Haines et al., 1998), we defined a curvilinear grid with variable knot-point spacing, to calculate a smoothed strain-rate in areas with few stations and a more detailed strain-rate where the distribution of GPS stations is dense. The estimated horizontal strain-rates are shown in Fig. 3.

In Fig. 3A, the arrows show the greatest extensional ($\dot{\varepsilon}_{Hma}$) and contractional ($\dot{\varepsilon}_{hmax}$) horizontal strain-rates, while the contours in the background show the magnitude of the dilatation strain-rate. The pattern clearly defines a contractional area along the northern rim of the plateau with a maximum negative strain-rate of ~0.2µstrain/yr. The maximum shortening strain rate direction (Fig. 3A) varies from N-S, along the north-eastern coastal border of the plateau, to NNW-SSE, along the limit of the foredeep. To the south, the shortening partially looses its strength and there is a slow transition to an extensional domain in the central sector of the plateau itself where, from west to east, the axis shows a clear rotation from a NNW-SSE direction to a NE-SW, with a maximum extensional strain-rate of ~0.1µstrain/yr. Though data are sparse along the Scicli-Ragusa fault system, the strain-rate axes are close to 45° to the fault zone and oriented for left-lateral strike slip as expected (Catalano et al., 2008). This general pattern is confirmed by the dilatation strain-rate pattern (Fig. 3A), evidencing as a large part of the deformation is accommodated in a really narrow region (i.e. the Scordia-Lentini Graben).

The maximum shear strain-rate is reported in Fig. 3B as a contour in the background. Because the (two conjugate) maximum shear directions might provide a tool to identify active faults, since motion along faults is related to shear on those structures, we reported these directions as cross-lines (Fig. 3B). Higher maximum shear strain-rates are observed on the Scordia-Lentini Graben and along the northern sector of the Scicli-Ragusa fault system, partially overlapping with the areas of strong seismicity. Along the northern sector of the Scicli-Ragusa fault, a discrete striking agreement between the azimuths of focal planes computed for the investigated area (Musumeci et al., 2005) and the conjugate maximum shear directions can be easily observed (Fig. 3B).

DISCUSSION

Velocity and strain-rate fields of the Hyblean Plateau have been investigated through non-permanent and permanent GPS measurements collected between 1998.00 and 2009.78. The network coverage is good in the north-eastern sector of the plateau, while data within the plateau itself are sparse, so this geodetic dataset allows us to improve the knowledge about the deformation pattern acting only along the north-eastern part of the plateau.

The velocity field referred to a stable Eurasian frame indicates that a large part of the plateau is dominated by northward motion with an average velocity of about 5.4mm/yr according to a large, long-term tectonic structure (i.e. the Eurasia-Nubia convergence). Sites located close to the Gela-Catania Foredeep (EIIV, IP04, IM01), eastward of the Scicli-Ragusa fault system, show low velocity values (~2.0mm/yr) evidencing shortening localized across the foredeep (Fig. 4). Resulting strain-rate evidenced a contractional area (~0.2μstrain/yr) along the northern rim of the plateau, with prevailing contractional axes N-S-oriented. Recent geological and Interferometric Synthetic Aperture Radar (InSAR) data detected active shortening along an area extending about 25km across the foredeep from the Scordia-Lentini Graben to the lower southern slope of Mt. Etna (Monaco et al., 2002; Bousquet and Lanzafame, 2004; Borgia et al., 1992; Froger et al., 2001). In particular, geological data have showed that normal faults controlling the Scordia-Lentini Graben have been reactivated by reverse motion during the last 0.85Myr

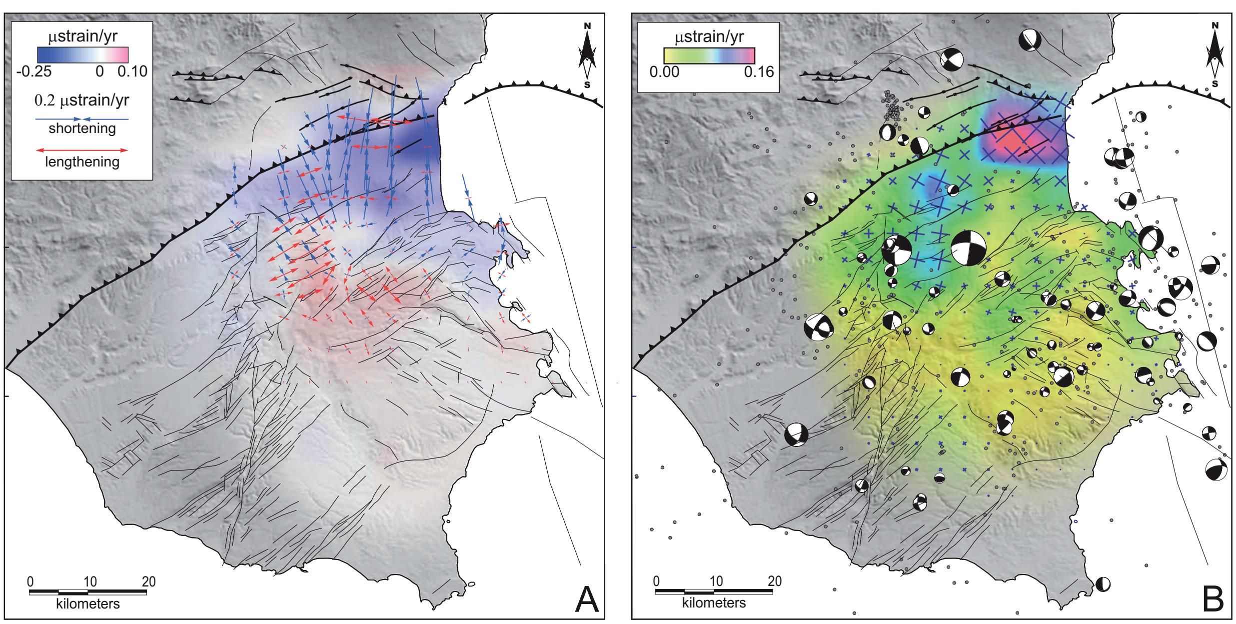

FIGURE 3 | **Geodetic strain-rate parameters: A) the contours in the background show the magnitude of the dilatation strain-rate while arrows represent the greatest extensional (red) and contractional (blue) horizontal strain-rates, B) the contours in the background show the magnitude of the maximum shear strain-rate, computed as** $\dot{\varepsilon}_{\max\_shear} = \frac{1}{2}\left(\dot{\varepsilon}_{H\max} - \dot{\varepsilon}_{h\min}\right)$ **, while black cross-lines represent its direction (and its perpendicular). Seismicity and focal mechanisms are also reported.**

(Catalano et al., 2008). In addition, InSAR data, mapping recent ground deformation patterns at Mt. Etna, have detected an active uplift of the ground along the line of sight of the satellite of a large anticline E-W-oriented extending for about 30km between the lower southern slope of the volcano and the Catania Plain (Borgia et al., 1992; Froger et al., 2001). Geological data have demonstrated that this compressional structure, deforming pre-Etnean sediments, has syn-sedimetary features (Lower-Middle Pleistocene age) related to the active compressive front of the chain (Monaco et al., 2002; Bousquet and Lanzafame, 2004). Our finding is in good agreement with both geological and InSAR data, mapping the contractional area across the Gela-Catania Foredeep with fine resolution and evidencing a still active compressive process. Considering the GPS velocity profile reported in Fig. 4, the total convergence rate can be estimated at about 4.4mm/yr along a direction parallel to the Eurasia-Africa convergence. This value is very high if compared with previous geodetic estimations for mainland Sicily (~1.0mm/yr; Doglioni et al., 2007 and references therein) but very close to the one estimated (~4.0mm/yr) to the north of Sicily (D'Agostino and Selvaggi, 2004). Considering that the RAFF station, which is located a few kilometers north of the foredeep, shows a velocity value close to the ones observed on the remain part of the plateau rather than to the ones observed across the foredeep, the following considerations can be done:

i) The contractional process is active only along the eastern sector of the Gela-Catania Foredeep; whereas along the western segment the contractional process is inactive; in this deformation picture, the Scicli-Ragusa fault system could play the role of a left-lateral transfer fault accommodating the contractional process across the eastern sector of the foredeep.

ii) The contractional process is transferred from the eastern sector of the foredeep to the north of Sicily across a transfer zone active in central Sicily (Fig. 5).

About the first point, the eastern sector of the Gela-Catania Foredeep is characterized by high values of maximum shear strain-rate (~0.16μstrain/yr), partially overlapping with the areas of occurrence of strong seismicity along the Scicli-Ragusa fault system. In addition, the strain-rate axes are close to 45° to the fault zone and oriented for left-lateral strike slip in agreement both with geological data (Catalano et al., 2008) and seismological data (i.e. focal mechanisms computed for strong earthquakes striking the area; Musumeci et al., 2005). In order to estimate the kinematic of the Scicli-Ragusa fault system, we applied a vectorial decomposition of the velocities of stations located across the fault. In particular, we estimated the rates of parallel (i.e. strike-slip) and perpendicular (i.e. tensile or opening) movement by taking into account velocity values at HVZN (located on the left of the fault system) and HMDC and IM02 stations (located on the right side of the system). RAFF station was excluded from this analysis because it is located north of the Gela-Catania Foredeep. Using a mean N10°E fault trend, we estimated a tensile and a strike-slip component of ca. 3mm/yr and ca. 1mm/yr (positive for left-lateral shear), respectively. We are aware that these values are estimated with very few stations, however they, coupled with seismological and geological data, indicate that the Scicli-Ragusa fault system could work as a left-lateral transfer fault accommodating the contractional process on the eastern sector of the foredeep as already supposed by Catalano et al. (2008). Anyway, the details of this tectonic picture are still being discussed and improvements in the spatial coverage of GPS stations on the entire Hyblean Plateau could better address this problem.

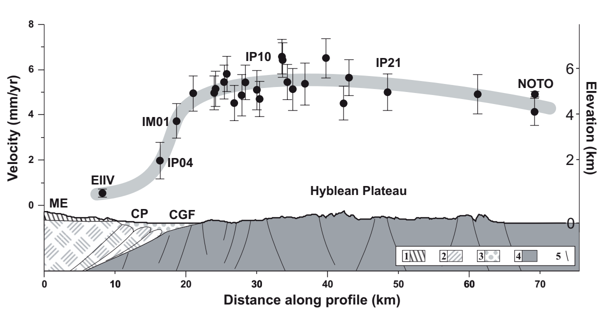

FIGURE 4 | **Horizontal velocity in the N20°W direction as a function of distance along the same direction. 1) Late Pleistocene-Holocene Etnean volcanics; 2) Appennine-Maghrebian units; 3) Recent-Quaternary sedimentary deposits; 4) Meso-Cenozoic carbonate sediments; 5) Main faults. ME: Mount Etna; CP: Catania Plain; CGF: Catania-Gela Foredeep.**

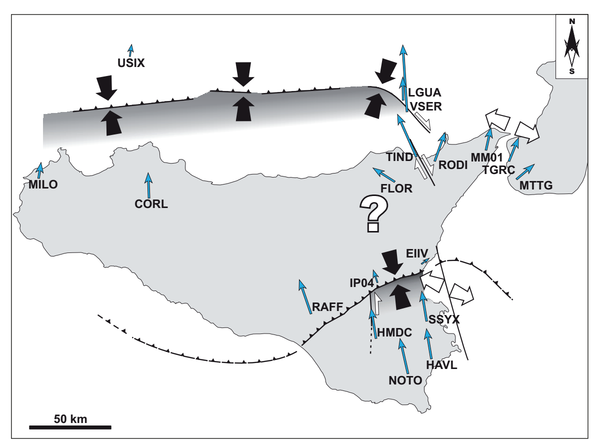

FIGURE 5 | **Large scale kinematic model of Sicily. GPS velocity relative to a fixed Eurasian frame are from i) this work (EIIV, IPO4, RAFF, HMDC, NOTO, HAVL, SSYX); ii) Mattia et al. (2008 and 2009) (LGUA, VSER, FLOR, RODI, MMO1, TIND, TGRC, MTTG) and iii) unpublished data (MILO, USIX CORL). See Table 1 for details.**

About the second point, despite the presence of two active contractional areas located respectively on the eastern sector of the Gela-Catania Foredeep (this study) and along northern Sicily (seismological and large-scale GPS data previously published; see Mattia et al. (2009), and references therein for details), there are neither geological nor seismological evidences about the presence of an active transfer zone in central Sicily. Again, the improvement of a denser and larger GPS network covering the whole of Sicily could also better address the problem here conjectured.

CONCLUSION

Based on the data presented here and discussed in the previous section, we may draw the following conclusions:

i) Velocity fields referred to a stable Eurasian frame indicate that a large part of the Hyblean Plateau is dominated by a 5.4mm/yr northward averaged velocity motion according to the Eurasia-Nubia convergence process.

ii) The strain-rate evidenced a contractional area along the northern rim of the plateau with a maximum negative strain-rate of ~0.2μstrain/yr (i.e. ~4.4mm/yr of convergence rate) in good agreement with both geological and InSAR data, evidencing a still active convergence process along this area.

iii) Though geodetic data are sparse along the Scicli-Ragusa fault system, our findings are in agreement with a possible movement as a left-lateral transfer fault accommodating the contractional process along the eastern sector of the foredeep.

iv) These findings coupled with previously published data, allow us to conjecture a transfer of a regional contractional process from the eastern sector of the foredeep to the north of Sicily across a transfer zone active in central Sicily. However, there are currently neither geological nor seismological evidences for the presence of an active transfer zone.

Main details of this tectonic picture are still being discussed and improvements in the spatial coverage of GPS stations on the whole of Sicily as planned by the Rete Integrata Nacionale di GPS and other important projects should better improve deformation process studies on the area.

ACKNOWLEDGMENTS

We thank Prof. Jesús Galindo Zaldívar and an anonymous referee for their reviews and comments that led to substantially improve the original version of the manuscript. We also thank M. Aloisi for constructive comments. In addition, we thank all those people involved in the field surveys in the Hyblean GPS network since 1998 and people involved in the maintenance of the permanent GPS station of the RING - Rete Integrata Nazionale GPS; in particular we wish to thank Giuseppe Puglisi, Alessandro Bonforte, Massimo Rossi, Daniele Pellegrino and Mario Pulvirenti. We thank S. Conway for correcting and improving the English of the paper.

REFERENCES

Adam, J., Grasso, M., Reuther, C.M., Torelli, L., 2000. Active fault kinematics and crustal stresses along the Ionian margin of southeastern Sicily. Tectonophysics, 326, 217-239.

Altamimi, Z., Collilieux, X., Legrand, J., Garayt, B., Boucher, C., 2007. ITRF2005: A new release of the International Terrestrial Reference Frame based on time series of station positions and Earth Orientation Parameters. Journal of Geophysical Research, 112, B09401. doi:10.1029/2007JB004949

Azzaro, R., Barbano, M.S., 2000. Analysis of the seismicity of Southeastern Sicily: a proposed tectonic interpretation. Annals of Geophysics, 43, 171-188.

Barberi, F., Gasparini, P., Innocenti, F., Villari, L., 1973. Volcanism of the southern Tyrrhenian Sea and its geodynamics implications. Journal of Geophysical Research, 78(23), 5221-5232.

Bianca, M., Monaco, C., Tortorici, L., Cernobori, L., 1999. Quaternary normal faulting in southeastern Sicily (Italy): a seismic source for the 1693 large earthquake. Geophysical Journal International, 139, 370-394.

Bird, P., 2003. An updated digital model of plate boundaries. Geochemistry Geophysics Geosystems, 4(3), 1027. doi:10.1029/2001GC000252

Boccaletti, M., Manetti, P., 1978. The Tyrrhenian sea and adjoining regions. In: Nairn, A.E.M. et al., Nairn, W.H.M., Kanes, W.H., Stehli, F.G, (eds.). The Ocean Basins and Margins. New York, Plenum Press, 4B, 149-200.

Bonforte, A., Anzidei, M., Puglisi, G., Mattia, M., Campisi, O., Casula, G., Galvani, A., Pesci, A., Puglisi, B., Gresta, S., Baldi, P., 2002. GPS surveys in the foreland-foredeep tectonic system of southeastern Sicily: first results. Annals of Geophysics, 45, 673-682.

Borgia, A., Ferrari, L., Pasquarè, G., 1992. Importance of gravitational spreading in the tectonic and volcanic evolution of Mount Etna. Nature, 357, 231-235.

Bousquet, J.C., Lanzafame, G., 2004. Compression and Quaternary tectonic inversion on the Northern edge of the Hyblean Mountains, foreland of the Appenine-Maghrebian chain in Eastern Sicily (Italy): geodynamic implications for Mt. Etna. GeoActa, 3, 165-177.

Catalano, S., De Guidi, G., Lanzafame, G., Monaco, C., Torrisi, S., Sturiale, G., Tortorici, G., Tortorici, L., 2006. Inversione tettonica positiva tardo-quaternaria nel Plateau Ibleo (Sicilia

SE). In Italian. Rendiconti Società Geologica Italiana, 2 Nuova Serie, 118-120.

Catalano, S., De Guidi, G., Romagnoli, G., Torrisi, S., Tortorici, G., Tortorici L., 2008. The migration of plate boundaries in SE Sicily: Influence on the large-scale kinematic model of the African promontory in southern Italy. Tectonophysics, 449, 41-62. doi:10.1016/j.tecto.2007.12.003

D'Agostino, N., Selvaggi, G., 2004. Crustal motion along the Eurasia-Nubia plate boundary in the Calabrian Arc and Sicily and active extension in the Messina Straits from GPS measurements. Journal of Geophysical Research, 109, B11402. doi:10.1029/2003TC001506

D'Agostino, N., Avallone, A., Cheloni, D., D'Anastasio, E., Mantenuto, S., Selvaggi, G., 2008. Active tectonics of the Adriatic region from GPS and earthquake slip vectors. Journal of Geophysical Research, 113, B12413. doi:10.1029/2008JB005860

Doglioni, C., Gueguen, E., Harabaglia, P., Mongelli, F., 1999. On the origin of W-directed subduction zones and applications to the western Mediterranean. In: Durand, B., Jolivet, L., Horvàth, F., Séranne, M. (eds.). The Mediterranean Basins: tertiary Extension within the Alpine Orogen. London, Geological Society, Special Publications, 156, 541-561.

Doglioni, C., Carminati, E., Cuffaro, M., Scrocca, D., 2007. Subduction kinematics and dynamic constraints. Earth-Science Reviews, 83, 125-175. doi:10.1016/j.earsirev.2007.04.001

Froger, J.L., Merle, O., Briole, P., 2001. Active spreading and regional extension at Mount Etna imaged by SAR interferometry. Earth and Planetary Science Letters, 187, 245-258.

Ghisetti, F., Vezzani, L., 1980. The structural features of the Iblean plateau and of the Monte Iudica area (South Eastern Sicily). A microtectonic contribution to the deformational history of the Calabrian. Bollettino della Società Geologica Italiana, 99, 57-102.

Grasso, M., Reuther, C.D., 1988. The western margin of the Hyblean Plateau: a neotectonic transform system on the SE Sicilian foreland. Annales Tectonicae, 2, 107-120.

Grasso, M., Philps, B., Reuther, C.D., Garofalo, P., Stamilla, R., Anfuso, G., Donzella, G., Cultrone, G., 2000. Pliocene–Pleistocene tectonics on western margin of the Hyblean plateau and the Vittoria Plain (SE Sicily). Memorie Società Geologica Italiana, 55, 35-44.

Haines, A.J., Jackson, A., Holt, W.E., Agnew, D.C., 1998. Representing distributed deformation by continuous velocity fields. Wellington (New Zeland), Science Report 98/5, Institute of Geology and Nuclear Science.

Haines, A.J., Holt, W.E., 1993. A procedure for obtaining the complete horizontal motions within zones of distributed deformation from the inversion of strain rate data. Journal of Geophysical Research, 98, 12,057-12,082.

Herring, T.A., King, R.W., McKlusky, S.C., 2006a. GAMIT reference manual: GPS Analysis at MIT, Version 10.3. Cambridge (Massachusetts), Massachusetts Institute of Technology, 1-171.

Herring, T.A., King, R.W., McKlusky, S.C., 2006b. GLOBK reference manual: Global Kalman filter VLBI and GPS Analysis Program, Version 10.3. Cambridge (Massachusetts), Massachusetts Institute of Technology, 1-95.

Hollenstein, C., Kahle, H.G., Geiger, A., Jenny, S., Goes, S., Giardini, D., 2003. New GPS constraints on the Africa-Eurasia plate boundary zone in southern Italy. Geophysical Research Letters, 30(18), 1935. doi:10.1029/2003GL017554

Holt, W.E., Haines, A.J., 1995. The kinematics of northern South Island, New Zealand, determined from geologic strain rates. Journal of Geophysical Research, 100(17), 991-18010.

Mattia, M., Palano, M., Bruno, V., Cannavò, F., 2009. Crustal motion along the Calabro-Peloritan Arc as imaged by twelve years of measurements on a dense GPS network. Tectonophysics, 476, 528-537. doi:10.1016/j.tecto.2009.06.006

Mattia, M., Palano, M., Bruno, V., Cannavò F., Bonaccorso, A., Gresta, S., 2008. Tectonic features of the Lipari–Vulcano complex (Aeolian archipelago, Italy) from 10 years (1996–2006) of GPS data. Terra Nova, 20, 370-377. doi:10.1111/j.1365-3121.2008.00830

Monaco, C., Bianca, M., Catalano, S., De Guidi, G., Tortorici, L., 2002. Sudden change in the Late Quaternary tectonic regime in eastern Sicily: evidences from geological and geomorphological features. Bollettino della Società Geologica Italiana, 1(special edition), 901-913.

Mulargia, F., Achilli, V., Broccio, F., Baldi, P., 1991. Is a destructive earthquake imminent in Southeastern Sicily? Tectonophysics, 188, 399-402.

Musumeci, C., Patanè, D., Scarfì, L., Gresta, S., 2005. Stress directions and shear-wave anisotropy: observations from local earthquakes in Southeastern Sicily, Italy. Bulletin of the Seismological Society of America, 95, 1359-1374.

Patacca, E., Sartori, R., Scandone, P., 1990. Thyrrenian basin and Apenninic arcs: kinematic relations since Late Tortonian times. Memorie Società Geologica Italiana, 45, 425-451.

Reuther, C.D., Ben-Avraham, Z., Grasso, M., 1993. Origin and role of major strike-slip transfers during plate collision in the Central Mediterranean. Terra Nova, 5, 249-257.

Scarfì, L., Giampiccolo, E., Musumeci, C., Patanè, D., Zhang H., 2007. New insights on 3D crustal structure in Southeastern Sicily (Italy) and tectonic implications from an adaptive mesh seismic tomography. Physics of the Earth Planetary Interiors, 161, 74-85.

Serpelloni, E., Vannucci, G., Pondrelli, S., Argnani, A., Casula, G., Anzidei, M., Baldi, P., Gasparini, P., 2007. Kinematics of the western Africa-Eurasia plate boundary from focal mechanisms and GPS data. Geophysical Journal International, 169, 1180-1200. doi: 10.1111/j.1365-246X.2007.03367.x

Yellin-Dror, A., Grasso, M., Ben-Avraham, Z., Tibor, G., 1997. The subsidence history of the northern Hyblean Plateau margin Eastern Sicily. Tectonophysics, 282, 277-289.

Manuscript received April 2010;
revision accepted April 2011;
published Online June 2011.